

Ionization probabilities of $A^2\Sigma^+(v'=0,1,2)$ and $B^2\Pi(v'=0,2)$ states of NO

H. Zacharias,^{a)} F. de Rougemont,^{b)} T. F. Heinz,^{c)} and M. M. T. Loy^{d)}

IBM Research Division, T. J. Watson Center Research Center, Yorktown Heights, New York 10598

(Received 29 January 1996; accepted 27 March 1996)

Ionization probabilities of NO molecules electronically excited in the $A^2\Sigma^+$ and $B^2\Pi$ states have been determined by (1+1) resonance-enhanced, two-photon ionization. Various vibrational levels within these states have been excited prior to ionization. Measurements of the unsaturated ionization signal yields accurate values for the relative detection probabilities of NO of 1:(0.70±0.07): (0.67±0.11) for excitation via the $\gamma(0-0)$, $\gamma(1-1)$, and $\gamma(2-2)$ bands, respectively, and $(3.7±0.36)×10^{-7}$ and $(5.8±0.65)×10^{-4}$ for ionization through $\beta(0-0)$ and $\beta(2-1)$ bands, respectively. Applying published data for the γ - and β -band transition probabilities allows the deduction of the ionization cross section of $A^2\Sigma^+$ and $B^2\Pi$ vibrational states. The respective ionization cross sections are $(7.0±0.9)×10^{-19}$ cm², $(8.5±0.8)×10^{-19}$ cm², $(6.0±1.0)×10^{-19}$ cm² for $A^2\Sigma^+(v'=0, 1, \text{ and } 2)$ and $(5.0±0.5)×10^{-21}$ cm² and $(1.7±0.2)×10^{-20}$ cm² for $B^2\Pi(v'=0 \text{ and } 2)$. These values are based on the experimentally determined cross section for $A^2\Sigma^+(v'=0)$. Using a larger theoretical cross section for this state the other cross sections scale accordingly, within the experimental uncertainties. © 1996 American Institute of Physics. [S0021-9606(96)01225-1]

I. INTRODUCTION

Resonance enhanced multiphoton ionization (REMPI) has been widely applied for sensitive detection of molecules at low concentration.¹ In investigations of various dynamical molecular effects, such as photodissociation, gas-phase reactions, and molecule/surface interactions, this process has been used as a spectroscopic method to deduce the rovibrational population distribution of the product molecules. For quantitative measurements REMPI requires detailed knowledge of both excitation steps, i.e., of the first step from the initial state to an intermediate bound electronic state and of the second step in which molecules in the excited state are ionized. For the first step, which yields the state selectivity of the technique, a wealth of spectroscopic data on transition energies and rovibronic line strengths is available. However, only a few theoretical or experimental studies deal with the transition leading from the excited state to ionization.² In some cases, such as the ionization of the $A^2\Sigma^+$ state of NO or the $B^1\Sigma^+$ state of CO, it has been found experimentally that the ionization cross section σ_1 is, to a large extent, independent of the rotational quantum number. In other molecules, like the $B^1\Sigma_u^+$ and $E,F^1\Sigma_g^+$ state of H₂, a strong variation of σ_1 with the intermediate rotational state is observed.^{3,4} The influence of vibrational excitation of an intermediate state on the ionization cross section has not been studied systematically, but is presumed to be observable in most molecules.

In this contribution, we report relative ionization probabilities of single rotational states in different vibrational levels of the $A^2\Sigma^+$ and $B^2\Pi$ states of NO. The measurements have been performed by means of (and at wavelengths appropriate for) the single-color (1+1) REMPI process involving $A^2\Sigma^+←X^2\Pi\gamma(0-0)$, $\gamma(1-1)$, and $\gamma(2-2)$ and $B^2\Pi←X^2\Pi\beta(0-0)$ and $\beta(2-1)$ bands. The results are required to infer accurate vibrational population distributions for NO in its ground electronic state from (1+1) REMPI spectra.

II. EXPERIMENT

The experiments are performed in an ultra-high vacuum ionization cell with a base pressure of about $3×10^{-8}$ mbar. The cell is equipped with sapphire windows brazed to a CF 35 flange. It can be uniformly heated up to 500 K, and the temperature is controlled by a thermocouple. In order to detect transitions originating from the sparsely populated $X^2\Pi(v''=2)$ level it is necessary to reduce nonresonant ionization of contaminants in the commercially available NO gas. This purification is accomplished by first passing the gas through a line cooled in pentane slush (144 K), and then subjecting it to repeated freezing and thawing cycles between 77 K and an acetone slush (178 K). The experiments are carried out at an NO density of $4.4×10^{-3}$ [amagat], corresponding to a pressure of about 4.4 mbar at room temperature, at various temperatures between 295 K and 450 K.

Radiation from an excimer laser pumped dye laser is frequency doubled in a β -BaB₂O₄ crystal to yield light tunable from 218 to 228 nm. This radiation has a spectral bandwidth of 0.4 cm⁻¹, a pulse energy of 15 μ J and a pulse duration of 15 ns. During frequency scanning accurate phase matching of the frequency doubling crystal is maintained by a servo device. The emerging UV beam is enlarged by an afocal lens system to a parallel beam of 2×5 mm² cross

^{a)}Permanent address: Fachbereich Physik, Universität Essen, 45117 Essen, Germany.

^{b)}On leave from Laboratoire d'Optique Quantique, Ecole Polytechnique, Palaiseau, France.

^{c)}Present address: Department of Physics, Columbia University, New York, New York 10027.

^{d)}Present address: Department of Physics, Hong Kong University of Science and Technology, Clear Water Bay, Kowloon, Hong Kong.

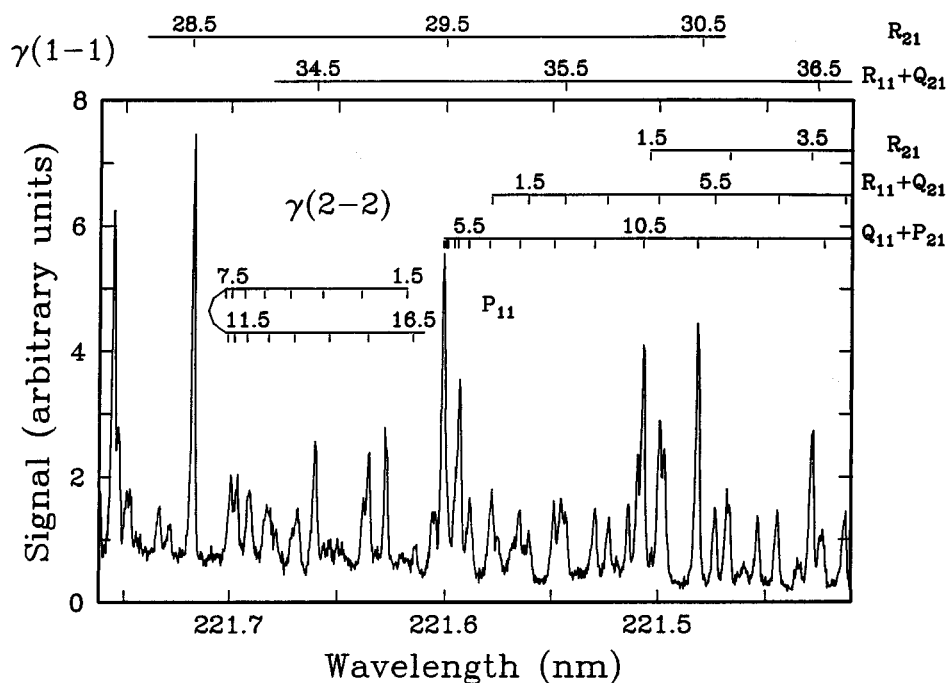


FIG. 1. Part of the NO $A\ ^2\Sigma^+(v'=2) \leftarrow X\ ^2\Pi(v''=2)$ $\gamma(2-2)$ band transition. Spectral resolution: 0.4 cm^{-1} , density: 4.34×10^{-3} amagat, cell temperature: $T=335\text{ K}$.

section with a fairly homogeneous spatial intensity distribution. The fluence of the UV beam is thus sufficiently low (0.15 mJ/cm^2) to avoid saturation effects in either excitation step. This is confirmed by the observed quadratic dependence of the ion signal on the laser fluence.

NO^+ ions generated are collected by a large metal plate (potential: $+100\text{ V}$ to ground), so that no gas amplification occurs. The collected charge is then electronically amplified, fed to a gated integrator, and stored in a microprocessor. The signal is normalized on a shot-to-shot basis to the square of the laser intensity. Depending on the signal strengths up to 30 pulses are averaged on each laser frequency setting. After such a measurement cycle the microprocessor advanced the laser frequency through actuating a stepping motor which turned the grating of the dye laser.

III. RESULTS

At room temperature REMPI spectra on NO could be detected only for the $\gamma(0-0)$, $\gamma(1-1)$, and $\beta(0-0)$ bands. At this temperature the vibrational population of NO in $X\ ^2\Pi(v''=2)$ is only about 1.7×10^{-8} of the ground state population. The rotationally state resolved population in this state could be observed via the $\gamma(2-2)$ band at 222 nm with good signal-to-noise ratio at cell temperatures of 335 K ($N_{v=2}=1.1 \times 10^{-7}$) and 450 K ($N_{v=2}=6.6 \times 10^{-6}$). A part of the experimental (1+1) REMPI spectrum of this band is shown in Fig. 1 together with an identification of the rotational lines. For a given vibrational level, rotational state populations can be derived from the measured spectra and the known Hönl–London rotational line strength factors for intermediate coupling.⁵ These population distributions are

found to be Boltzmann for all three vibrational levels $v''=0,1$, and 2 , with a temperature matching that of the cell. This result confirms that the ionization cross section of the $A\ ^2\Sigma^+$ state does not have a significant dependence on the degree of rotational excitation.

The dependence of the ionization probability on the vibrational level in the $A\ ^2\Sigma^+$ state can be established by comparing the ionization signal obtained from the $\gamma(0-0)$, $\gamma(1-1)$, and $\gamma(2-2)$ band. Due to the similarity of the upper and lower state electronic potential energy curves these transitions occur in the same wavelength region. Within a single wavelength scan lines of all three transitions are observed, minimizing systematic errors in the measurement.

By scanning the wavelength of the laser to shorter wavelengths, red degraded β bands of the $B\ ^2\Pi \leftarrow X\ ^2\Pi$ transition appear. We observe rotationally resolved lines of the $\beta(0-0)$ band with the R_{11} band head at about 219.825 nm and of the $\beta(2-1)$ band with the R_{11} band head at 219.08 nm , which are shown in Fig. 2. The rotational line position of these β bands are assigned from molecular constants given by Lagerqvist and Miescher.⁶ Since in the same wavelength region as the medium J'' lines of the $\beta(0-0)$ band the $\gamma(2-2)$ band appears with its well-known energetic position, a precise determination of the electronic excitation energy of the B state could in principle be performed, as was recently obtained for the $\beta(3-0)$ band.⁷

IV. DATA ANALYSIS

The relative ionization probabilities of single rotational levels of different vibrational states in $A\ ^2\Sigma^+$ are obtained by comparing the heights of corresponding rotational lines from

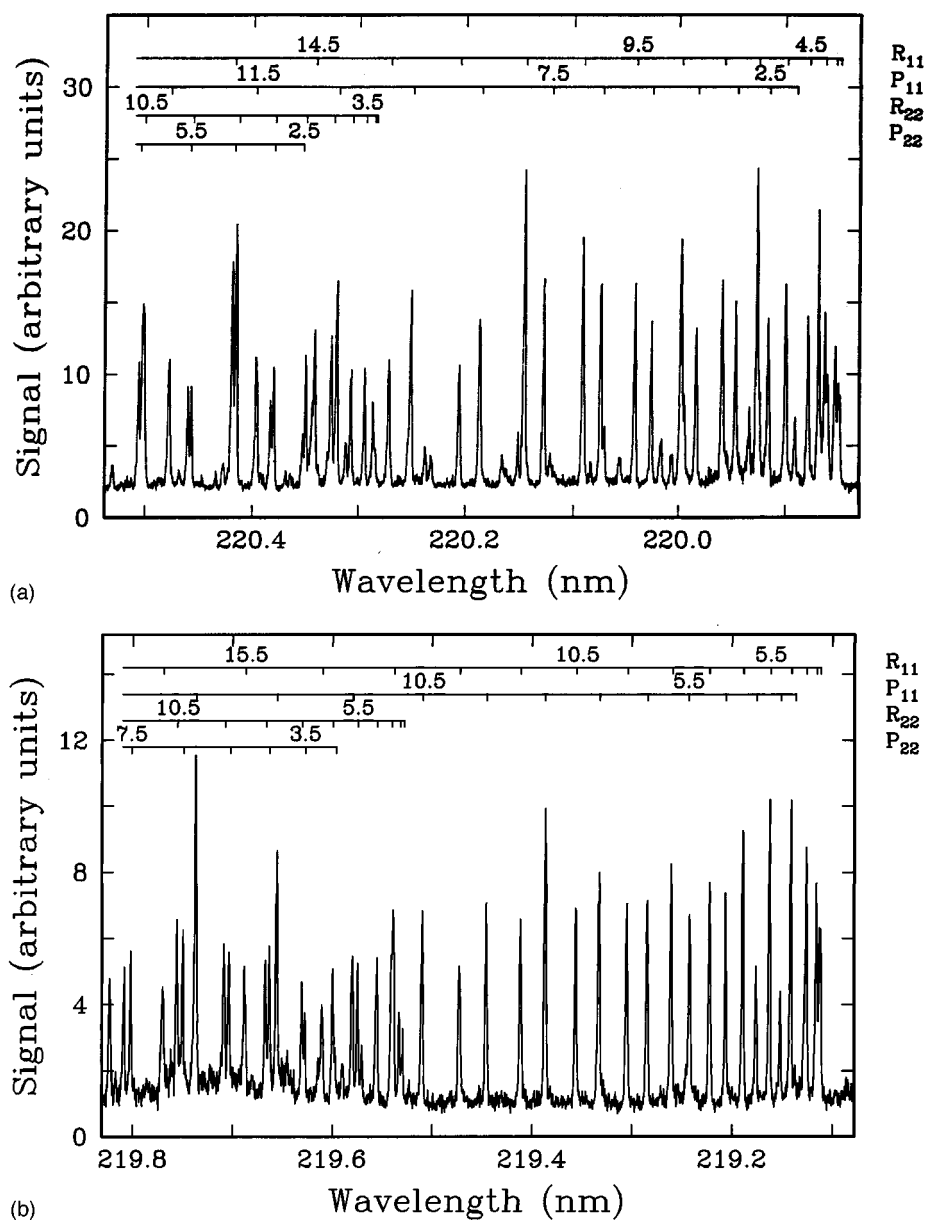


FIG. 2. (a) Part of the NO $B^2\Pi(v'=0) \leftarrow X^2\Pi(v''=0)$ $\beta(0-0)$ band spectrum. The lines of the $\beta(0-0)$ band are identified in the upper part of the figure. The small unidentified lines belong to the $\beta(2-1)$ band. Other conditions as in Fig. 1. (b) Part of the NO $B^2\Pi(v'=2) \leftarrow X^2\Pi(v''=1)$ $\beta(2-1)$ band. Other conditions as in (a).

the respective spectra. In order to minimize the influence of possible alignment effects⁸ only lines belonging to the same rotational branches are compared, in this case P_{11} and $(R_{11} + Q_{21})$. Since in the cell an equilibrated sample is studied, which can be characterized by a temperature, the results for different J'' can be averaged after the level degeneracy $(2J'' + 1)$ and the Boltzmann factor $\exp[-E_{\text{int}}/kT]$ have been properly taken into account.

For resonantly enhanced two-photon ionization, relaxation in the intermediate state has to be considered.^{9,10} In molecular systems this relaxation can be separated into a rate γ , which repopulates the initial level, and a rate α , which removes the particular molecule from the ensemble during the exciting laser pulse. Depending on the particular molecu-

lar system, often many rovibrational levels are accessible for the relaxation from the intermediate states. In that case the rate γ can largely be neglected compared to α . For the system under consideration, namely NO, $A^2\Sigma^+$, $v'=(0,1,2)$ and $B^2\Pi$, $v'=(0,2)$, γ is determined by the vibrational and rotational branching ratios. In the case of NO half of the fluorescence is emitted to the other spin-orbit manifold of the electronic ground state. Taking the vibrational branching ratios from a recent determination of the Einstein coefficients¹¹ a repopulation rate γ is calculated (for $J''=9.5$) to be of the order of, but less than, $2.0 \times 10^5 \text{ s}^{-1}$, $1.2 \times 10^5 \text{ s}^{-1}$, and $1.7 \times 10^5 \text{ s}^{-1}$, for the $\gamma(0-0)$, $\gamma(1-1)$, and $\gamma(2-2)$ bands, respectively, when $(R_{11} + Q_{21})$ and $(P_{21} + Q_{11})$ rotational branches are excited. This rate is small compared to α (see

TABLE I. Transition frequencies $\tilde{\nu}_{v',v''}$, Einstein coefficients $A_{v',v''}$, upper state lifetimes $\tau_{v'}$, and electronic self-quenching rates k_q for some β and γ bands of NO. Inspecting results of different authors an uncertainty of the quenching rates of about $\pm 10\%$ for the A state and about $\pm 7.5\%$ for the B state is estimated.

$v' - v''$	$\tilde{\nu}_{v',v''}$ [cm ⁻¹]	$A_{v',v''}$ [s ⁻¹]	$\tau_{v'}$ [ns]	k_q [10 ⁻¹⁰ cm ³ s ⁻¹]			
				$T=295$ K	335 K	405 K	450 K
A $^2\Sigma^+$							
0-0	44204	1.00×10^6 ^a	202 ^a	2.30 ^b	2.45	2.69	2.84
1-1	44670	5.90×10^5 ^a	192 ^a	2.03 ^b	2.16	2.38	2.51
2-2	45131	8.52×10^5 ^a	182 ^a	1.75 ^b	1.86	2.05	2.16
B $^2\Pi$							
0-0	45485	34 ^c	2000 ^d	2.67 ^e	2.47 ^g		
2-1	45637	1.58×10^4 ^f	1520 ^d	2.80 ^e	2.59 ^g		

^aReference 11.

^bReference 15.

^cReferences 24 and 32.

^dReference 32.

^eReference 21.

^fEstimated from ground state absorption f values (Ref. 24) and theoretical Franck–Gordon factors (Refs. 25 and 26), see text.

^gEstimated from Ref. 16.

Table II) and is thus neglected in the following analysis. For emission from the B $^2\Pi$ state the corresponding ratio of the rates γ and α is even smaller due to the valence character of the B state, which causes most emission to high vibrational levels of the X $^2\Pi$ state.

With this simplification the measured ion yield n_I is given by¹⁰

$$n_I(v', v'') = n_0(v'') \frac{W_2(v')}{W_2(v') + \alpha(v')} \left\{ 1 + \frac{x-y}{2y} \times e^{-(x+y)\Delta t} - \frac{x+y}{2y} e^{-(x-y)\Delta t} \right\}, \quad (1)$$

where

$$x = (2W_1(v', v'') + W_2(v') + \alpha(v'))/2, \quad (1a)$$

and

$$y = [W_1^2(v', v'') + \frac{1}{4}(W_2(v') + \alpha(v'))^2]^{1/2}. \quad (1b)$$

Δt denotes the laser pulse width, and $n_0(v'')$ the rovibrational population in the electronic ground state. The ion yield measured depends on the excitation rate $W_1 = \sigma_1 I_1 / \hbar \omega_1$, the ionization rate $W_2 = \sigma_I I_2 / \hbar \omega_2$, and the intermediate state relaxation rate α , all three of which depend on the particular intermediate vibrational level v' in the A $^2\Sigma^+$ state. In general, a reduction of the excitation cross section σ_1 due to a broadening of the intermediate state by the relaxation rate α and the ionization rate W_2 has to be taken into account.¹⁰ For our experimental conditions, however, this broadening is negligibly small.

The quantity we want to evaluate is the relative magnitude of the ionization rates $\sigma_I(v')$ for the three different vibrational levels of the A $^2\Sigma$ state, $v'=0,1,2$, and for $v'=0,2$ of the B $^2\Pi$ state. For this purpose it is useful to discuss the different relaxation rates occurring in the intermediate state. The relaxation rate α is the sum of the fluorescence decay rate τ^{-1} and the electronic quenching rate $R_q = k_q \times [\text{NO}]$,

where k_q denotes the quenching rate constant and $[\text{NO}]$ the NO concentration in the cell. Rotational state selective measurements of the fluorescence lifetimes have been performed, e.g., Refs. 12 and 13. For consistency reasons we take the weighted values published by Piper and Cowles,¹¹ although their lifetime values for A $^2\Sigma^+$, $v'=0$ is 10% smaller than the earlier measured and generally accepted value.^{12,13} Also the electronic self-quenching rate constant k_q has been measured rotational state selectively, although only at room temperature.^{12,14} Here we take the data published by Imajo *et al.*¹⁵ Their ($v'=0$) rate agrees well with more recent determinations of the electronic quenching rate of this state.¹⁶⁻¹⁸ They also provide data for ($v'=1$) and ($v'=2$) of the A state. The rates for $v'=0$ and 1 are 10% and 30% larger than earlier measurements.^{12,14} Recently, the electronic quenching rate for A $^2\Sigma^+$, $v'=0$ has also been measured in heated cells^{16,18} and shock tubes¹⁷ as a function of temperature. For NO as collision partner these experiments confirm the independence of the collision cross section on temperature.¹⁹ The deactivation rate k_q thus scales with the average relative velocity of the NO molecules: $k_q = \sigma_q \langle v \rangle$.

Electronic quenching rates for the B $^2\Pi$ state have been determined by Melton and Klemperer²⁰ and recently by Crosley and co-workers.^{16,21} In contrast to the A state the collisional cross section of the B state decreases with temperature.¹⁶ For the present work we estimate the cross section at $T=335$ K from the measured cross section at 295 and 550 K. The value of Raiche and Crosley at 295 K is also much larger than the earlier one.²⁰ We thus performed a separate determination of the ionization cross section of this state using the quenching rates of Melton and Klemperer. We thereby find that the resulting ionization cross section changes only within the error bars of the present experiment. The Einstein coefficients, lifetimes, and electronic quenching rate constants used in this work are summarized in Table I.

Besides electronic quenching to the ground state, energy

TABLE II. Total intermediate state relaxation rate α at a NO density of 4.34×10^{-3} [amagat] and the excitation rate W_1 of the intermediate state (laser pulse energy 15 μ J) in the ($R_{11} + Q_{21}$) branch for the $A^2\Sigma^+$ state and in the P_{11} branch for the $B^2\Pi$ state.

$v' - v''$	$\alpha [10^7 \times s^{-1}]$				$W_1 [s^{-1}]$			
	$T=295$ K	335 K	405 K	450 K	$J''=10.5$	29.5	33.5	36.5
$A^2\Sigma^+$								
0-0	2.95	3.12	3.37	3.53	5.37 E6	4.53 E6	4.42 E6	4.34 E6
1-1	2.69	2.83	3.07	3.20	3.07 E6	2.59 E6	2.53 E6	2.48 E6
2-2	2.42	2.54	2.74	2.86	4.29 E6	3.63 E6	3.54 E6	3.48 E6
$B^2\Pi$								
					$J''=7.5$	16.5	21.5	
0-0	2.90	2.69			2.61 E2	2.55 E2	2.55 E2	
2-1	3.06	2.83			1.20 E5	1.17 E5	1.17 E5	

transfer processes within the vibrational levels of the excited state and to other electronic states also have to be considered. In both cases the molecules are not lost for the ionization step but experience a different ionization probability than in the originally excited state. Melton and Klemperer²⁰ determined the vibrational relaxation rate constant in $A^2\Sigma^+$ to be $(1.4 \pm 1.1) \times 10^{-11} \text{ cm}^3 \text{ s}^{-1}$ for $v' = 2 \rightarrow v' = 1$ and also for $v' = 2 \rightarrow v' = 0$; a similar value is obtained for $v' = 1 \rightarrow v' = 0$. These rate constants are more than an order of magnitude smaller than the electronic quenching rates. Since the molecules are not lost but are ionized just with a slightly different ionization cross section, this pathway is not considered separately in the analysis. The energy transfer between different electronic states proceeds with even smaller rate constants,²⁰ being $(8 \pm 1) \times 10^{-12} \text{ cm}^3 \text{ s}^{-1}$ and $(4 \pm 2) \times 10^{-12} \text{ cm}^3 \text{ s}^{-1}$ for $A^2\Sigma^+(v' = 1) \rightarrow B^2\Pi(v' = 0)$ and $B^2\Pi(v' = 3) \rightarrow A^2\Sigma^+(v' = 0)$, respectively. More recent studies arrive at similar values.^{21,22} These rates are therefore also neglected.

The total quenching rate of the intermediate state is then

$$\alpha = k_q[\text{NO}] + \tau^{-1}. \quad (2)$$

Using the parameters in Table I we then calculate for a density of 4.34×10^{-3} [amagat] (=4.34 mbar at room temperature) total deactivation rates α as listed in Table II. Also given in Table I are the Einstein $A_{v'v''}$ coefficients¹¹ for absorption of the first photon from the $X^2\Pi$ to the intermediate state. From these coefficients the effective absorption cross section $\sigma_{J'J''}^{v'v''}$ of a single rovibronic line can be derived from²³

$$f_{v'v''} = \frac{mc\lambda^2}{8\pi^2 e^2} A_{v'v''}, \quad (3)$$

$$f_{J'J''} = \frac{S_{J'J''}}{2J'' + 1} f_{v'v''}, \quad (4)$$

$$\sigma_{J'J''}^{v'v''} = \frac{\pi e^2}{mc} \frac{2\sqrt{\ln 2}}{\sqrt{\pi}} f_{J'J''} \frac{1}{\Delta\nu}, \quad (5)$$

where $S_{J'J''}$ denotes the Hönl–London factor of the transition and $\Delta\nu$ gives the convolution of the Doppler width and the Gaussian bandwidth of the exciting laser light, in the

approximation when this bandwidth is large compared to the natural line width. The other factors have their usual meaning. One obtains

$$\sigma_{J'J''}^{v'v''} = \frac{\lambda^2}{8\pi} \frac{2\sqrt{\ln 2}}{\sqrt{\pi}} \frac{S_{J'J''}}{2J'' + 1} \frac{1}{\Delta\nu} A_{v'v''}, \quad (6)$$

where the Hönl–London factors include the electronic degeneracy when they are calculated in the intermediate (a)–(b) coupling.⁵ It should be mentioned that neither experimental nor theoretical Einstein coefficients for the $\beta(2-1)$ band are available. We thus estimate its value from the measured oscillator strength of the $\beta(2-0)$ band²⁴ and theoretical Franck–Condon factors.^{25,26} Thereby we assume a constant electronic transition moment $R_e(\bar{r}_{v'v''})$, which approximately holds for these two transitions.²⁷

With this effective rovibronic excitation cross section the excitation rate $W_1 = \sigma_{J'J''}^{v'v''} I_1 / \hbar \omega_1$ can be calculated for the intermediate states $A^2\Sigma^+(v' = 0, 1, 2)$ and $B^2\Pi(v' = 0, 2)$. (See Table II). The ionization cross sections of these intermediate states are then obtained by calculating the ion yield expected for the experimental conditions. For $A^2\Sigma^+(v' = 0)$ both an experimental ionization cross section of $\sigma_I^{\text{exp}} = 7.0 \times 10^{-19} \text{ cm}^2$ (Ref. 28) and a theoretical cross section $\sigma_I^{\text{th}} = 1.158 \times 10^{-18} \text{ cm}^2$ (Ref. 2) are adopted. Although the experimental value was determined for an ionization wavelength of 266 nm, it has been used successfully also for the ionization wavelength of ~ 226 nm in (1+1) REMPI experiments.^{9,29} A similar insensitivity of the ionization cross section on the wavelength is also observed in one photon ionization for the same total excitation energy region.^{30,31} This independence on the wavelength is supported by the theoretical calculations.² For the other intermediate states the ionization cross sections have been numerically varied until the experimentally observed intensity ratios to the $\gamma(0-0)$ band are fitted best. The results thus obtained are summarized in Table III. Finally, Table IV lists the relative ionization probabilities of NO for two-photon ionization through β and γ bands, when both excitation and ionization steps are not saturated. The values hold for a laser intensity of 10 kW/cm². The relative values are only marginally influenced by intermediate state electronic quenching.

TABLE III. Ionization cross sections of NO $A^2\Sigma^+$ ($v'=0,1,2$) and $B^2\Pi$ ($v'=0,2$) (I): based on the experimental value for σ_I ($A^2\Sigma^+$, $v'=0$)= 7.0×10^{-19} cm² (Ref. 28). (II): based on the theoretical value for σ_I ($A^2\Sigma^+$, $v'=0$)= 1.158×10^{-18} cm² (Ref. 39). (2σ) standard deviations are given.

	λ_I [nm]	E_{exc} [cm ⁻¹]	(I): σ_I [cm ²]	(II): σ_I [cm ²]
$A^2\Sigma^+$				
$v'=0$	266.05 ^a	7202	$(7.0\pm 0.9)\times 10^{-19}$	1.158×10^{-18}
	226.0 ^b	13 863		
$v'=1$	223.58	16 807	$(8.5\pm 0.8)\times 10^{-19}$	$(1.4\pm 0.2)\times 10^{-18}$
$v'=2$	221.30	19 574	$(6.0\pm 1.0)\times 10^{-19}$	$(1.0\pm 0.2)\times 10^{-18}$
$B^2\Pi$				
$v'=0$	220.09	16 350	$(5.0\pm 0.5)\times 10^{-21}$	$(8.3\pm 0.5)\times 10^{-21}$
$v'=2$	219.36	18 529	$(1.7\pm 0.2)\times 10^{-20}$	$(2.8\pm 0.3)\times 10^{-20}$
$v'=7$	354.7	5 863.7	$(8.0\pm 2.0)\times 10^{-20}$ ^c	

^aReference 28.

^bReferences 9 and 29.

^cReference 10.

V. DISCUSSION

Determinations of absolute ionization cross sections of electronically excited molecular states have been rarely performed so far, either experimentally or theoretically.³³ In general, the experimental difficulties are caused by the necessity to gather absolute numbers of the intermediate state population and the number of ions generated, in conjunction with a good knowledge about the temporal and spatial laser beam profile. Such absolute numbers are not required when the saturation method^{34,35} is used, where the intensity of the ionizing laser radiation is increased until this transition is saturated. Since molecular ionization cross sections are often in the 10^{-18} to 10^{-20} cm² range, this requires fluences of 0.75 to 75 J/cm² and more, which should be variable independently from the exciting laser intensity. The method thus requires a second laser beam, with the imponderabilities of a highly reproducible beam overlap. To our best knowledge experimental measurements of molecular excited state ionization cross sections have been performed only for NO $A^2\Sigma^+$,²⁸ $H_2 E, F^2\Sigma_g^+$,³⁶ $H_2 B^2\Sigma_u^+$,³ and NO $B^2\Pi$, $C^2\Pi$, and $D^2\Sigma$.¹⁰

A theoretical calculation of ionization cross sections in molecules is hampered by the multitude of autoionization and dissociative channels open even at only moderate photon excess energies. All channels may contribute with different relative phase to the total cross section. In a series of papers

McKoy and co-workers calculated ionization cross sections for various molecules, including H_2 and NO .²

Whereas earlier calculations for $H_2 B^1\Sigma_u^+$ neglected the autoionization channel in H_2 ,^{37(a)} known to be extremely important,³⁸ this contribution was later included for the $C^1\Pi$ state.^{37(b)} They also reported theoretical cross sections for NO $A^2\Sigma^+$ ($v'=0$) for various ionization conditions.³⁹ They obtained a value of about $\sigma_I=1.158\times 10^{-18}$ cm² for an ionization wavelength of $\lambda_I=225$ nm. In the range $\lambda_I=225$ to 324 nm only a slight variation of this cross section from $\sigma_I=1.158\times 10^{-18}$ cm² to $\sigma_I=1.135\times 10^{-18}$ cm² was found.³⁹ This cross section is about a factor of 2 larger than the earlier determined experimental one of $\sigma_I^{\text{exp}}=7.0\times 10^{-19}$ cm²,²⁸ determined with the saturation method, which requires a good knowledge of the laser beam cross section.

For the $A^2\Sigma^+$ state the variation of the ionization cross section with the intermediate vibrational state is relatively weak (Table III). The reason for this insensitivity is due to the Rydberg character of the A state, which consist of nearly 94% of s , 5.4% of d , and only 0.6% of higher angular momentum states.³⁹ The Franck–Condon factors thus strongly favor $\Delta v=0$ transitions. The nearly pure $3p\sigma$ angular momentum also favors $\Delta N=0$ rotational transitions from the A state to the $NO^+ X$ state.⁴⁰

The ionization cross sections of the B state are expectedly lower than those for the A state, because the ionization involves a valence-Rydberg excitation with a change of two electron orbitals: $\dots(\sigma 2p)^2(\pi 2p)^3(\bar{\pi} 2p)^2 \rightarrow \dots(\sigma 2p)^2(\pi 2p)^4 + e^-$. The values of $\sigma_I^B(v'=0)=5.0\times 10^{-21}$ cm² and $\sigma_I^B(v'=2)=1.7\times 10^{-20}$ cm² are in accord with an earlier determined one for the $v'=7$ state of $\sigma_I^B(v'=7)=8\times 10^{-20}$ cm².¹⁰ The overlap of the vibrational wave function of the B state with final levels in the $X^1\Sigma^+$ ion state increases with the vibrational quantum number, yielding thus larger ionization cross sections.

For the NO $A^2\Sigma^+$ state very detailed investigations of the ionization dynamics have been performed by Zare and co-workers.⁴⁰ After preparation of single m_j states in $A^2\Sigma^+$ ($v'=0$) photoelectron angular distributions for ionization into specific final rotational states of $NO^+ X^1\Sigma^+$

TABLE IV. Experimentally derived relative ionization probabilities for (1+1) REMPI. Laser intensity: 10 kW/cm².

$v'-v''$	λ_{vac} [nm] ^a	$p=4.34$ mbar	$p=0$
$A^2\Sigma^+$			
0-0	226.22	1.0	1.0
1-1	223.86	(0.71 ± 0.07)	(0.70 ± 0.07)
2-2	221.58	(0.69 ± 0.11)	(0.67 ± 0.11)
$B^2\Pi$			
0-0	219.85	$(3.6\pm 0.36)\times 10^{-7}$	$(3.7\pm 0.36)\times 10^{-7}$
2-1	219.11	$(5.6\pm 0.65)\times 10^{-4}$	$(5.8\pm 0.65)\times 10^{-4}$

^a R_{11} bandhead.

have been measured. These experiments show that rotational alignment effects in the intermediate state in resonantly enhanced two-photon ionization are important. To minimize the influence of such effects on the relative total ionization cross section for different intermediate vibrational states we thus compared line intensities always in the same rotational branches, mostly ($R_{11} + Q_{21}$) and P_{11} .

The quantities measured in this work are the relative ionization probabilities via $v' = 0, 1$, and 2 in the NO $A\ 2\Sigma^+$ state (Table IV). The ionization cross sections are values derived from this measurement by making use of other excitation probabilities taken from the literature. The two quantities which enter directly into this calculation are the relative electronic transition moments for the $A-X$ excitation step and the ionization cross section of the $A\ 2\Sigma^+(v'=0)$ level. To account for the two known cross sections of this state—the experimental one²⁸ and the theoretical one³⁹—Table III gives the derived cross sections for $v'=1$ and $v'=2$ for both in columns four and five, respectively. As is seen these values scale nearly linearly with this reference value. For the electronic transition moments we used the compilation of Piper and Cowles.¹¹ The other quantities which enter this calculation—laser fluence, intermediate state lifetimes and quenching rates of the A state levels—are of less importance for the measurements of the relative ionization probabilities. Numerical simulations show that even a change of the laser fluence by a factor of 2 in both direction changes in this case the ionization cross section by only a few percent. Changes in the quenching cross section are of similar weak influence as the laser power, since both the reference ionization via the $\gamma(0-0)$ band and the pathway with unknown ionization cross section are effected in a similar way by the intermediate state quenching. In addition the ionization via the A and B states takes place within 5 ns, whereas the average deactivation time at the pressures employed is about 30 to 40 ns (see Table II).

The relative ionization probabilities via the $B\ 2\Pi(v'=0$ and $2)$ levels can experimentally be linked to those via the $A\ 2\Sigma^+$ state, because the $\beta(2-1)$ and $\beta(0-0)$ bands occur in the same wavelength region as the $\gamma(2-2)$ band. The largest uncertainty for the value of the $B\ 2\Pi(v'=0$ and $2)$ ionization cross section comes again from uncertainties of the Franck–Condon factor, especially the very low value for the $\beta(0-0)$ band. A recent measurement of the lifetimes of the vibrational levels $v'=0$ to 6 of the B state by Gadd and Slanger³² is on the other hand in very good agreement with the oscillator strengths of the $B-X$ transitions²⁴ which relate to the Franck–Condon factors.

¹S. H. Lin, Y. Fujimura, H. J. Neusser, and E. W. Schlag, *Multiphoton Spectroscopy of Molecules* (Academic, Orlando, 1984).

²S. N. Dixit and V. McKoy, *J. Chem. Phys.* **82**, 3546 (1985); V. McKoy, M. Braunstein, H. Rudolf, J. A. Stephens, S. N. Dixit, and D. L. Lynch, *J. Electron Spectrosc. Rel. Phenom.* **52**, 597 (1990).

³W. Meier, H. Rottke, H. Zacharias, and K. H. Welge, *J. Chem. Phys.* **83**, 4360 (1985); W. Meier, H. Rottke, and H. Zacharias, *Inst. Phys. Conf. Ser.* **94**, 93 (1988).

- ⁴W. M. Huo, K. D. Rinnen, and R. N. Zare, *J. Chem. Phys.* **95**, 205 and 214 (1991).
- ⁵R. J. Bennett, *Mon. Not. R. Astron. Soc.* **147**, 35 (1970).
- ⁶A. Lagerqvist and E. Miescher, *Helv. Phys. Acta* **31**, 221 (1958); *Can. J. Phys.* **44**, 1525 (1966).
- ⁷G. W. Faris and P. C. Cosby, *J. Chem. Phys.* **97**, 7073 (1992).
- ⁸D. C. Jacobs and R. N. Zare, *J. Chem. Phys.* **85**, 5457 (1986).
- ⁹W. G. Mallard, J. H. Miller, and K. C. Smyth, *J. Chem. Phys.* **76**, 3483 (1982).
- ¹⁰H. Rottke and H. Zacharias, *J. Chem. Phys.* **83**, 4831 (1985); **84**, 7058 (1986).
- ¹¹L. G. Piper and L. M. Cowles, *J. Chem. Phys.* **85**, 2419 (1986).
- ¹²H. Zacharias, J. B. Halpern, and K. H. Welge, *Chem. Phys. Lett.* **43**, 41 (1976).
- ¹³I. S. McDermid and J. B. Laudenslager, *J. Quant. Spectrosc. Radiat. Transfer* **27**, 483 (1982).
- ¹⁴M. Asscher and Y. Haas, *Chem. Phys. Lett.* **59**, 231 (1978); *J. Chem. Phys.* **76**, 2115 (1982).
- ¹⁵T. Imajo, K. Shibuya, K. Obi, and I. Tanaka, *J. Phys. Chem.* **90**, 6006 (1986).
- ¹⁶G. A. Raiche and D. R. Crosley, *J. Chem. Phys.* **92**, 5211 (1990).
- ¹⁷J. A. Gray, P. H. Paul, and J. L. Durant, *Chem. Phys. Lett.* **190**, 266 (1992).
- ¹⁸M. C. Drake and J. W. Ratcliffe, *J. Chem. Phys.* **98**, 3850 (1993).
- ¹⁹P. H. Paul, J. A. Gray, J. L. Durant, Jr., and J. W. Thoman, Jr., *Appl. Phys. B* **57**, 249 (1993).
- ²⁰L. A. Melton and W. Klemperer, *J. Chem. Phys.* **59**, 1099 (1973).
- ²¹J. Luque and D. R. Crosley, *J. Chem. Phys.* **100**, 7340 (1994).
- ²²R. J. Cattolica, T. G. Mataga, and J. A. Cavolowsky, *J. Quant. Spectrosc. Radiat. Transfer* **42**, 499 (1989).
- ²³R. W. Nicholls, in *Physical Chemistry, An Advanced Treatise*, edited by H. Eyring, D. Henderson, and W. Jost (Academic, London, 1969) Vol. 3, p. 325.
- ²⁴V. Hasson and R. W. Nicholls, *J. Phys. B: Atom Molec. Phys.* **4**, 1769 (1971).
- ²⁵H. A. Ory, A. P. Gittleman, and J. P. Maddox, *Astrophys. J.* **139**, 346 (1964).
- ²⁶R. W. Nicholls, *J. Res. Nat. Bur. Std.* **68A**, 535 (1964).
- ²⁷D. M. Cooper, *J. Quant. Spectrosc. Rad. Transfer* **27**, 459 (1982).
- ²⁸H. Zacharias, R. Schmiedl, and K. H. Welge, *Appl. Phys.* **21**, 127 (1980).
- ²⁹D. C. Jacobs, R. J. Madix, and R. N. Zare, *J. Chem. Phys.* **85**, 5469 (1986).
- ³⁰K. Watanabe, F. M. Matsunaga, and H. Sakai, *Appl. Opt.* **6**, 391 (1967).
- ³¹Y. Ono, S. H. Linn, H. F. Prest, C. Y. Ng, and E. Miescher, *J. Chem. Phys.* **73**, 4855 (1980).
- ³²G. E. Gadd and T. G. Slanger, *J. Chem. Phys.* **92**, 2194 (1990).
- ³³V. S. Letokhov, *Laser Photoionization Spectroscopy* (Academic, Orlando, 1987).
- ³⁴R. V. Ambartzumian, N. P. Furzikov, V. S. Letokhov, and A. A. Puretsky, *Appl. Phys.* **9**, 335 (1976).
- ³⁵U. Heinzmann, D. Schinkowski, and H. D. Zeman, *Appl. Phys.* **12**, 113 (1977).
- ³⁶D. J. Kliger, J. Bokor, and C. K. Rhodes, *Phys. Rev. A* **21**, 607 (1980).
- ³⁷(a) H. Rudolf, D. L. Lynch, S. N. Dixit, and V. McKoy, *J. Chem. Phys.* **84**, 6657 (1986); (b) S. N. Dixit, D. L. Lynch, B. V. McKoy, and A. U. Hazi, *Phys. Rev. A* **40**, 1700 (1989).
- ³⁸Ch. Jungen, O. Atabek, *J. Chem. Phys.* **66**, 5584 (1977); S. Ross and Ch. Jungen, *Phys. Rev. A* **50**, 4618 (1994) and references therein.
- ³⁹H. Rudolf, S. N. Dixit, V. McKoy, W. M. Huo, *J. Chem. Phys.* **88**, 1516 (1988); H. Rudolf, V. McKoy, and S. N. Dixit, *J. Chem. Phys.* **90**, 2570 (1989); S. N. Dixit, D. L. Lynch, V. McKoy, and W. M. Huo, *Phys. Rev. A* **32**, 1267 (1985).
- ⁴⁰S. W. Allendorf, D. J. Leahy, D. C. Jacobs, and R. N. Zare, *J. Chem. Phys.* **91**, 2216 (1989); D. J. Leahy, K. L. Reid, R. N. Zare, *ibid.* **95**, 1757 (1991); D. J. Leahy, K. L. Reid, H. Park, and R. N. Zare, *ibid.* **97**, 4948 (1992); H. Park and R. N. Zare, *ibid.* **99**, 6537 (1993).